Cancer Research
cancerres.aacrjournals.org

doi: 10.1158/0008-5472.CAN-06-0504
Cancer Res August 1, 2006 66; 7420

Epigenetic Inactivation of the Dioxin-Responsive *Cytochrome P4501A1* Gene in Human Prostate Cancer

Steven T. Okino[1], **Deepa Pookot**[1], **Long-Cheng Li**[1], **Hong Zhao**[1], **Shinji Urakami**[1], **Hiroaki Shiina**[2], **Mikio Igawa**[2], and **Rajvir Dahiya**[1]

+ Author Affiliations

Requests for reprints:
Steven T. Okino, Department of Urology, San Francisco Veterans Affairs Medical Center, 4150 Clement Street, San Francisco, CA 94121. Phone: 415-221-4810, ext. 3509; Fax: 415-750-6639; E-mail steveokino@gmail.com.

Abstract

2,3,7,8-Tetrachlorodibenzo-*p*-dioxin (TCDD; dioxin) is a toxic environmental contaminant that works through dioxin response elements (DRE) to activate gene expression. We tested the hypothesis that cancer-related epigenetic changes suppress dioxin activation of the *cytochrome P4501A1* (*CYP1A1*) gene. 5-Aza-2′-deoxycytidine (5-aza-CdR), an inhibitor of DNA methylation, increases TCDD-inducible *CYP1A1* mRNA expression in cancerous LNCaP cells but not in noncancerous PWR-1E and RWPE-1 cells (all human prostate cell lines). Bisulfite DNA sequencing shows that the TCDD-responsive *CYP1A1* enhancer is highly methylated in LNCaP cells but not in RWPE-1 cells. *In vivo* footprinting experiments reveal that unmethylated DRE sites do not bind protein in response to TCDD in LNCaP cells, whereas inducible DRE occupancy occurs in RWPE-1 cells. Pretreatment of LNCaP cells with 5-aza-CdR partially restores TCDD-inducible DRE occupancy, showing that DNA methylation indirectly suppresses DRE occupancy. Chromatin immunoprecipitation experiments reveal that LNCaP cells lack trimethyl histone H3 lysine 4, a mark of active genes, on the *CYP1A1* regulatory region, whereas this histone modification is prevalent in PWR-1E and RWPE-1 cells. We also analyzed *CYP1A1* enhancer methylation in human prostate tissue DNA. We do not detect *CYP1A1* enhancer methylation in 30 DNA samples isolated from noncancerous prostate tissue. In contrast, 11 of 30 prostate tumor DNA samples have detectable *CYP1A1* enhancer methylation, indicating that it is hypermethylated in prostate tumors. This is the first report that shows that *CYP1A1* is aberrantly hypermethylated in human prostate cancer and has an altered, inaccessible chromatin structure that suppresses its dioxin responsiveness. (Cancer Res 2006; 66(15): 7420-8) (Cancer Res 2006; 66(15): 7420-8)

CYP1A1 **TCDD** **CpG methylation** **human** **prostate cancer**

Introduction

DNA methylation, the covalent addition of a methyl group to the 5-carbon of cytosine in a CpG dinucleotide, is an epigenetic event that suppresses gene expression. In the human genome, CpG sites are often clustered in structures termed CpG islands that are located in the regulatory region of

many genes. In normal cells, most CpG islands are unmethylated and associated with active genes or genes capable of active transcription. In cancerous cells, CpG islands often become hypermethylated, leading to aberrant gene silencing (1– 3).

2,3,7,8-Tetrachlorodibenzo-*p*-dioxin (TCDD; also called dioxin) is a notorious environmental contaminant that produces toxic, neoplastic, and reproductive effects in experimental animals (4, 5) and poses an unclear risk to human health (6). The most well-studied dioxin response is the transcriptional induction of the *cytochrome P4501A1* (*CYP1A1*) gene. TCDD induces *CYP1A1* by binding to and activating the aryl hydrocarbon receptor (AhR), which then translocates to the nucleus and interacts with its partner protein Arnt to form an active heteromeric transcription factor (termed AhRC for AhR complex). AhRC interacts with DNA-binding sites, termed dioxin response elements (DRE), located on the *CYP1A1* enhancer to mediate TCDD-inducible gene expression (7). All DRE sites contain a CpG dinucleotide (8), which, when methylated *in vitro*, inhibits AhRC binding in an electrophoretic mobility shift assay and suppresses TCDD-inducible reporter gene activity (9, 10). These findings suggest that methylation of the *CYP1A1* enhancer may suppress its TCDD responsiveness.

A study analyzing lung tissue shows that *CYP1A1* is methylated in humans (11). *CYP1A1* methylation is also observed in human and rabbit cells grown in culture (10, 12). Here, we study the influence of DNA methylation and chromatin structure on dioxin action and *CYP1A1* expression in cancerous and noncancerous human prostate cell lines and tissue samples. We find that the *CYP1A1* enhancer is aberrantly hypermethylated in prostate cancer and has an altered, inaccessible chromatin structure that suppresses its dioxin responsiveness.

Materials and Methods

Cells and cell culture. PWR-1E, RWPE-1, and LNCaP cells were obtained from the American Type Culture Collection (Manassas, VA) and cultured as directed. For the *in vivo* footprint and RNA analysis experiments, cells were split on day 0 and treated with 5-aza-2′-deoxycytidine (5-aza-CdR; Sigma, St. Louis, MO) starting on day 1 at a dose of 0.25 or 1.0 μmol/L. Culture medium was changed on day 4, and fresh 5-aza-CdR was added. Cells were treated with TCDD (10 nmol/L; Wellington Laboratories, Inc., Guelph, Ontario, Canada) on day 6 for 18 hours or on day 7 for 2 hours. Total RNA and genomic DNA were isolated on day 7 using the RNeasy Mini kit or the DNeasy Tissue kit (Qiagen, Valencia, CA), respectively, following the manufacturer's directions. To analyze *CYP1A1* methylation, LNCaP cells were split on day 0 and treated with 1.0 μmol/L 5-aza-CdR starting on day 1. Culture medium was changed on day 4, and fresh 5-aza-CdR was added. Cells were split on day 7, and fresh 5-aza-CdR was added. Culture medium was changed on day 11, and fresh 5-aza-CdR was added. Genomic DNA was isolated on day 14 using the DNeasy Tissue kit.

Human prostate tissue samples. Thirty cancerous and 30 noncancerous human prostate samples were collected by radical prostatectomy and transurethral resection of the prostate, respectively, at the Shimane University School of Medicine (Shimane, Japan). Genomic DNA was isolated from the prostate samples using the QIAamp Tissue kit (Qiagen) following the manufacturer's directions.

Quantitation of mRNAs. Reverse transcription-PCR (RT-PCR) was done using the Titanium One-Step RT-PCR kit (BD Biosciences, San

Jose, CA) following the manufacturer's directions. *CYP1A1* mRNA was amplified using the primers 5′-CTGAATGCCTTCAAGGACCTGAATGAGA-3′ (forward) and 5′-GGTTTACAAAGACACAACGCCCCTTGG-3′ (reverse) using 30 cycles of 30 seconds at 94°C, 30 seconds at 65°C, and 1 minute at 72°C. AhR mRNA was amplified using the primers 5′-CTGAAGCAGAGCTGTGCACGAGAGG-3′ (forward) and 5′-AGACTGGACCCAAGTCCATCGGTTG-3′ (reverse) using 30 cycles of 30 seconds at 94°C, 30 seconds at 63°C, and 1 minute at 72°C. Arnt mRNA was amplified using the primers 5′-GCTGGGAGATCAGAGCAACAGCTACAA-3′ (forward) and 5′-TGTTTCTTTCCAGAGGGACTGCTCACA-3′ (reverse) using 30 cycles of 30 seconds at 94°C, 30 seconds at 63°C, and 1 minute at 72°C. Glyceraldehyde-3-phosphate dehydrogenase (G3PDH) mRNA was amplified using the primers 5′-TCCCATCACCATCTTCCA-3′ (forward) and 5′-CATCACGCCACAGTTTCC-3′ (reverse) using 30 cycles of 30 seconds at 94°C, 30 seconds at 60°C, and 1 minute at 72°C. The amplified DNA was electrophoresed on a 2% agarose gel and visualized by staining with ethidium bromide.

Bisulfite DNA sequencing. Bisulfite modification of genomic DNA was done using the CpGenome DNA Modification kit (Chemicon, Temecula, CA) following the manufacturer's directions. Primers for bisulfite genomic sequencing PCR were designed manually or by using the online program MethPrimer (http://www.urogene.org/methprimer/). All primer sequences lack CpG sites and thus amplify methylated and unmethylated DNA equivalently. Bisulfite-modified DNA was amplified using two rounds of PCR using nested primers. Sequences of the primers are as follows: CYP1A1-1, 5′-CTCTTAAAACCTAAAATCACAAAAATC-3′ (forward); CYP1A1-2, 5′-AAATTCCAAAAAACTATCACCTTCA-3′ (forward); CYP1A1-3, 5′-AACTAATCTCTCTAAAATTAAAAAA-3′ (forward); CYP1A1-4, 5′-AAAACACCTAAAAATCCCAATTCCA-3′ (forward) and 5′-TGGAATTGGGATTTTTAGGTGTTTT-3′ (reverse); CYP1A1-5, 5′-CTTAAAAAAAAAATCCCAAAACAACCC-3′ (forward) and 5′-GGGTTGTTTTGGGTATTTTTTTTTAAG-3′ (reverse); CYP1A1-6, 5′-AAACTAAACCTATCCCCCAAAACCC-3′ (forward) and 5′-GGGTTTTGGGGGATAGGTTTAGTTT-3′ (reverse); CYP1A1-7, 5′-ACCCTTAAAAATCCCTCTTAACTCC-3′ (forward) and 5′-GGAGTTAAGAGGGATTTTTAAGGGT-3′ (reverse); CYP1A1-8, 5′-CTTTAATTAACAAAACACAAAAATC-3′ (forward) and 5′-GATTTTTGTGTTTTGTTAATTAAAG-3′ (reverse); CYP1A1-9, 5′-TCCCTCTAAAAAACAAAAATCAAAC-3′ (forward) and 5′-GTTTGATTTTTGTTTTTTAGAGGGA-3′ (reverse); CYP1A1-10, 5′-AAACTCTTAAAAAACCAACCTC-3′ (forward) and 5′-GAGGTTGGTTTTTTAAGAGTTT-3′ (reverse); CYP1A1-11, 5′-ATACAAAAAATCTAAATCTAC-3′ (forward) and 5′-GTAGATTTAGATTTTTTGTAT-3′ (reverse); CYP1A1-12, 5′-AACCCCAATACCATTTAACATAACC-3′ (forward) and 5′-GGTTATGTTAAATGGTATTGGGGTT-3′ (reverse); CYP1A1-13, 5′-ACCTTCCTATTACAAAATTTCCAAA-3′ (forward) and 5′-TTTGGAAATTTTGTAATAGGAAGGT-3′ (reverse); CYP1A1-14, 5′-GAGGTGAGGGGATTATTTTTTGGTT-3′ (reverse); CYP1A1-14a, 5′-CTAATCCAAACCAAAAAATAATCCC-3′ (forward); CYP1A1-14b, 5′-AAATAATCCCCTCACCTCCCATTCC-3′ (forward); CYP1A1-15, 5′-TGTTTTTTTTTATTAGAATGTAAAT-3′ (reverse); CYP1A1-15b, 5′-GAGATTAGGAGTGTTGTTAGTTGTG-3′ (reverse); CYP1A1-16, 5′-TAGATTTGGGGTATATTATTTGTTT-3′ (reverse); and CYP1A1-17, 5′-TTGATTTTTTTGTTTTGAATTGTAA-3′ (reverse).

PCR conditions were as follows: 3 minutes at 94°C, 35 cycles of 1 minute at 94°C, 30 seconds at 56°C, and 1 minute at 72°C followed by 5 minutes at 72°C extension step. Second-round PCR was done using 1 μL of the first-round PCR product in a total volume of 50 μL. The amplification product was confirmed by electrophoresis on a 2% agarose gel and sequenced directly by an outside vendor (McLab, South San Francisco, CA).

Quantitation of CpG methylation. The methylation level of individual CpG sites on *CYP1A1* was estimated directly by comparing the height of the cytosine peak with the height of the thymine peak on the DNA sequencing chromatogram. A single cytosine peak was considered to represent 100% methylation; a single thymine peak was considered to represent no methylation. CpG sites with overlapping cytosine and thymine peaks were considered to be partially methylated. In the latter instance, the percentage of methylation was calculated as the ratio of the peak heights of the cytosine to cytosine plus thymine signals.

The methylation level of *CYP1A1* CpG sites 52 to 85 was also estimated by sequencing individual DNA strands. Bisulfite-modified DNA was amplified using primers CYP1A1-7 (forward) and CYP1A1-10 (reverse) in the primary reaction and primers CYP1A1-8 (forward) and CYP1A1-10 (reverse) in the secondary reaction. The PCR product was cloned into pSC-A using the StrataClone PCR Cloning kit according to the manufacturer's directions (Stratagene, La Jolla, CA). Individual clones were picked and grown, and plasmid DNA was isolated using the QIAprep Spin Miniprep kit (Qiagen) and sequenced by an outside vendor (McLab) using the T3 primer.

***In vivo* footprinting.** *In vivo* footprinting using dimethyl sulfate (DMS; Sigma) was done as described previously (13, 14). To analyze DRE 3, we used the following primer set: primer 1, 5′-TTCAATCAAGAGGCGCGAACCT-3′; primer 2, 5′-AACCTCAGCTAGTCGCCCGGGCTCT-3′; and primer 3, 5′-GTCCAGCCCCGCGGCGCCTCTGGCCTT-3′. To analyze DRE 6, we used the following primer set: primer 1, 5′-TTGCGTGAGAAGGACCGGAGG-3′; primer 2, 5′-CGCGCAGCCACCCAGCCGACCCATT-3′; and primer 3, 5′-AGCCACCCAGCCGACCCATTCCCCGGC-3′. To analyze DRE 10, we used the following primer set: primer 1, 5′-TTGGGGAGCACGTCGGGGAT-3′; primer 2, 5′-GTCGGGGATGGCGCGTAACGATGTT-3′; and primer 3, 5′-GGATGGCGCGTAACGATGTTAGCTGGG-3′. For primers 1, 2, and 3, the annealing temperatures were 50°C, 65°C, and 70°C, respectively.

Chromatin immunoprecipitation assay. Confluent PWR-1E, RWPE-1, and LNCaP cells were treated with TCDD (10 nmol/L) for 90 minutes or left untreated. The cells were then harvested for chromatin immunoprecipitation (ChIP) analysis using the EZ-ChIP kit (Upstate Biotechnology, Charlottesville, VA) according to the manufacturer's directions. Antibodies used in the immunoprecipitations were purchased from Upstate Biotechnology and recognized acetyl histone H3, acetyl histone H4, dimethyl histone H3 lysine 4, trimethyl histone H3 lysine 4, and dimethyl histone H3 lysine 9. The immunoprecipitated DNA was eluted in a total volume of 50 μL. DNA (2 μL) was analyzed by PCR using the following conditions: 3 minutes at 94°C, 28 cycles of 30 seconds at 94°C, 30 seconds at 63°C, and 30 seconds at 72°C followed by 5 minutes at 72°C extension step. The amplified DNA was electrophoresed on a 3% agarose gel and visualized by staining with

ethidium bromide. The sequence of the primers used in the ChIP analysis were as follows: promoter, 5′-CCGCCACCTTTCTCTCCAATCCCAG-3′ (forward) and 5′-ATAGGCGGGCTTGTACGTGTGGCCA-3′ (reverse); DRE 3, 5′-TCAGGGCTGGGGTCGCAGCGCTTCT-3′ (forward) and 5′-GCTACAGCCTACCAGGACTCGGCAG-3′ (reverse); DRE 4, 5′-TGACCTCTGCCCCCTAGAGGGATGT-3′ (forward) and 5′-TTGGCAGAGCACAGAAATCCGGCGG-3′ (reverse); DRE 5 to 6, 5′-TTTAAGAGCCCCGCCCCGACTCCCT-3′ (forward) and 5′-CAGGCGTTGCGTGAGAAGGACCGGA-3′ (reverse); DRE 10, 5′-GTCGGGGATGGCGCGTAACGATGTT-3′ (forward) and 5′-CCTCCGGAACCTTCCTGTTACAGGG-3′ (reverse); upstream, 5′-AAGGCCTTCCCTGACCCCCTTGTTT-3′ (forward) and 5′-GCTGACAGCACTCCTAATCTCGTGG-3′ (reverse); and G3PDH, 5′-TACTAGCGGTTTTACGGGCGCACGT-3′ (forward) and 5′-TCGAACAGGAGGAGCAGAGAGCGAA-3′ (reverse).

Results

Effect of 5-aza-CdR on *CYP1A1* expression. 5-Aza-CdR, a nucleotide analogue that demethylates genomic DNA, is commonly used to determine if DNA methylation influences gene expression (15, 16). We treated two noncancerous human prostate cell lines (PWR-1E and RWPE-1) and one cancerous human prostate cell line (LNCaP) with 5-aza-CdR to assess its effect on constitutive and TCDD-inducible *CYP1A1* mRNA expression. Our results (Fig. 1) reveal striking differences between the cancerous and noncancerous cell lines. Both of the noncancerous cell lines exhibit low basal *CYP1A1* expression that is dramatically increased following TCDD exposure. 5-Aza-CdR has little effect on constitutive or TCDD-induced *CYP1A1* expression. This pattern of *CYP1A1* expression is consistent with its expression in most healthy animal tissues and, thus, is considered normal. In contrast, in the cancerous LNCaP cells, basal *CYP1A1* expression is not detectable and is only barely detectable in cells exposed to TCDD. 5-Aza-CdR dramatically increases the TCDD inducibility of *CYP1A1* in a dose-dependent fashion; no effect on constitutive *CYP1A1* expression is observed (Fig. 1). This pattern of *CYP1A1* expression is aberrant and suggests that cancer-associated DNA methylation suppresses TCDD induction of *CYP1A1*.

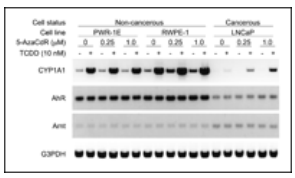

View larger version:
In this page In a new window
Download as PowerPoint Slide

Figure 1.

Effect of 5-aza-CdR on *CYP1A1* mRNA expression in human prostate cell lines. Total RNA was isolated from the indicated cell lines and analyzed by RT-PCR using primers specific for *CYP1A1*, AhR, Arnt, and *G3PDH*. Cells were treated with 5-aza-CdR at the indicated doses for 7 days and/or TCDD (10 nmol/L) for 18 hours. RT-PCR reactions were separated by electrophoresis on a 2% agarose gel and stained with ethidium bromide. This experiment was repeated thrice with similar results.

Our results imply that, in LNCaP cells, either the *CYP1A1* gene is suppressed directly by DNA methylation or the dioxin response system is suppressed by DNA methylation. Suppression of the dioxin response

system may be accomplished by inactivation of either of its two main components, AhR or Arnt. To determine if AhR or Arnt is regulated by DNA methylation, we analyzed their mRNA levels in the prostate cell lines (Fig. 1). We find that AhR is expressed at a lower level and Arnt is expressed at a slightly higher level in LNCaP cells relative to the noncancerous cell lines. 5-Aza-CdR has little effect on AhR or Arnt expression in all cells. We conclude that DNA methylation does not significantly influence AhR or Arnt expression in LNCaP cells. We therefore infer that direct methylation of *CYP1A1* likely suppresses its TCDD inducibility.

CpG islands on the *CYP1A1* enhancer. In human cancers, CpG sites are often hypermethylated, resulting in aberrant suppression of gene expression (1, 2). CpG sites that affect gene expression are typically located in CpG islands in gene regulatory regions. To identify CpG islands on the *CYP1A1* gene locus (defined as 50 kb upstream and 25 kb downstream of the *CYP1A1* transcriptional start site), we analyzed it using "the CpG island searcher" developed by Takai and Jones (17). We find that only two CpG islands exist within this 75-kb region (Fig. 2*A*). One of the CpG islands (CpG island 2) is located between –2,813 and –3,567 bp upstream of the *CYP1A1* transcription start site; the function of this region is unknown. The other CpG island (CpG island 1) occurs between –178 and –1,712 bp upstream of the *CYP1A1* transcription start site. This region, previously identified as the *CYP1A1* enhancer, confers dioxin inducibility and contains all of the DRE sites that are implicated in dioxin induction of *CYP1A1* (Fig. 2*B*; refs. 7, 18). Thus, the dioxin-responsive *CYP1A1* enhancer is contained within a CpG island, a DNA region susceptible to DNA methylation.

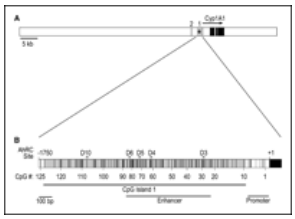

View larger version:
In this page In a new window
Download as PowerPoint Slide

Figure 2.

CpG islands on the CYP1A1 locus. *A,* CpG islands on the CYP1A1 gene locus were identified using the criteria of Takai and Jones (17). CpG islands are indicated by *gray boxes*. The *asterisk* represents the location of the TCDD-responsive CYP1A1 gene enhancer. *Black lines/boxes* represent CYP1A1 exons. The transcribed region of CYP1A1 and the direction of transcription is indicated. *B,* a schematic representation of CpG island 1 and flanking DNA is shown (+1 to –1,750 relative to the transcriptional start site). High-affinity AhRC binding sites identified previously by *in vivo* footprinting are labeled and indicated. AhRC binding sites are numbered consistent with a previous report (ref. 18; D10, DRE 10; D6, DRE 6, etc.). CpG sites are indicated by *black lines* and are numbered sequentially starting from the transcription start site and increasing in the upstream direction. The location of CpG island 1 (*gray shading*) and the *CYP1A1* enhancer and promoter are indicated. A portion of *CYP1A1* exon 1 is indicated by the *black box*.

***CYP1A1* gene methylation in cultured human prostate cells.** We next analyzed cell line DNA by direct bisulfite DNA sequencing to determine the methylation status of all CpG sites between +1 and –1,750 relative to

the *CYP1A1* transcriptional start site. This region contains 125 CpG sites, all of CpG island 1, and all known regulatory sites that affect *CYP1A1* gene expression (Fig. 2*B*; refs. 7, 18). In RWPE-1 cells (Fig. 3*B*), we do not detect methylation of CpG sites 1 to 90. Thus, in these noncancerous prostate cells, the entire *CYP1A1* regulatory region is unmethylated and is not constrained in its ability to control transcription. We detect methylation of CpG sites 91 to 125. However, this methylated DNA is upstream of the *CYP1A1* regulatory region and is not known to control gene expression. In LNCaP cells, we detect methylation of CpG sites 37 to 90 (Fig. 3*B*). These sites are not methylated in RWPE-1 cells and encompass the TCDD-responsive *CYP1A1* enhancer. We also find that the *CYP1A1* promoter is not methylated (CpG sites 1-36) and DNA upstream of the regulatory region of *CYP1A1* is highly methylated (CpG sites 91-125) in LNCaP cells. This pattern of DNA methylation is similar to that observed in RWPE-1 cells and suggests that these regions are not associated with the differential 5-aza-CdR sensitivity observed in our gene expression experiment (Fig. 1). Together, these results imply that cancer-dependent enhancer hypermethylation suppresses TCDD induction of *CYP1A1*.

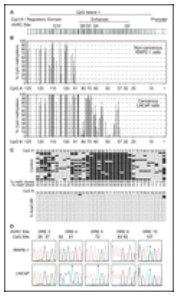

View larger version:
In this page In a new window
Download as PowerPoint Slide

Figure 3.

CYP1A1 gene methylation in cultured human prostate cells. *A*, a schematic representation of the *CYP1A1* gene depicting CpG sites (*black lines*), CpG island 1 (*gray shading*), the *CYP1A1* enhancer and promoter, and AhRC binding sites. *B*, the extent of methylation of each CpG site as determined by direct bisulfite DNA sequencing of RWPE-1 cell DNA and LNCaP cell DNA. *C,* the pattern and extent of *CYP1A1* enhancer methylation in control LNCaP cells and in LNCaP cells treated with 5-aza-CdR (1 μmol/L) for 14 days as determined by the sequencing of 20 individual DNA strands. *Black boxes* indicate methylated CpG sites, and *white boxes* indicate unmethylated CpG sites. The percentage of methylation of each CpG site in control LNCaP cells as estimated by the sequencing of individual DNA strands and the direct sequencing of PCR products is also shown. *D,* representative bisulfite DNA sequencing chromatograms analyzing DNA isolated from RWPE-1 cells and LNCaP cells. The portions of the sequencing chromatograms analyzing DREs 3 to 6 and DRE 10 are shown. The *blue lines* represent cytosine and indicates the presence of 5-methylcytosine; the *red lines* represent thymine and indicates the presence of thymine and unmethylated cytosine; the *green lines* represent adenine; the *black lines* represent guanine; *asterisks* indicates sites containing significant levels of 5-methylcytosine.

We also determined the methylation pattern on the *CYP1A1* enhancer in individual DNA strands by cloning the bisulfite PCR product into a plasmid vector and sequencing individual clones. As expected, no DNA

methylation was detected in 10 clones derived from RWPE-1 DNA and in 12 clones derived from PWR-1E DNA (data not shown). In contrast, all 20 clones derived from control LNCaP DNA exhibited a unique pattern of DNA methylation (Fig. 3*C*). Of the 34 CpG sites analyzed, the number of methylated sites ranged from 12 to 28 with an average of 18.4. Importantly, the percentage of methylation of each individual CpG site determined in this analysis was similar to that determined by direct sequencing of the PCR products (Fig. 3*C*). This serves to validate our method used to quantitate DNA methylation and clearly shows that, within the *CYP1A1* enhancer, individual CpG sites exhibit widely different levels of DNA methylation.

We also assessed *CYP1A1* enhancer methylation in LNCaP cells treated with 5-aza-CdR for 7 or 14 days. We find that cells treated for 7 days had ~15% less methylation than control cells (data not shown). Remarkably, in LNCaP cells treated with 5-aza-CdR for 14 days, the *CYP1A1* enhancer is almost entirely devoid of methylation. Of the 20 clones analyzed, 17 had no detectable DNA methylation and the other 3 clones were methylated at only a single CpG site (Fig. 3*C*). We conclude that the *CYP1A1* enhancer is sensitive to demethylation by 5-aza-CdR.

Effect of DNA methylation on protein-DNA interactions. Using *in vivo* footprinting procedures, Kress et al. (18) identified four functional DREs on the human *CYP1A1* enhancer (DREs 3-6). All of these DRE sites contain the high-affinity AhRC recognition motif 5′-TNGCGTG-3′ (8) A fifth DRE site (DRE 10), although containing a high-affinity AhRC recognition motif, was found to be nonfunctional because it did not bind protein *in vivo*. Other DRE sites (DREs 1-2 and DREs 7-9) lack a “T” residue in the first position of the recognition motif, have a lower affinity for AhRC, and are nonfunctional *in vivo* (8, 18).

Our DNA methylation results analyzing the high-affinity AhRC-binding sites reveal that DREs 3 and 6 are unmethylated in both LNCaP and RWPE-1 cells, DREs 4 and 5 are methylated in LNCaP cells but not in RWPE-1 cells, and DRE 10 is methylated in both LNCaP and RWPE-1 cell lines (Fig. 3*D*). To assess the functionality of these sites, we analyzed them by *in vivo* footprinting (Fig. 4). First, within the *CYP1A1* enhancer, we analyzed DREs 3 and 6, sites that are unmethylated in both LNCaP and RWPE-1 cells. As a positive control, we analyzed DRE occupancy in dioxin-responsive RWPE-1 cells. We find that TCDD induces dramatic changes in the DMS modification pattern of bases within the DREs. One base exhibits TCDD-inducible DMS hypersensitivity, and two other bases exhibit TCDD-dependent DMS hyposensitivity (Fig. 4*A* and *B*). This pattern of DMS modification reflects TCDD-inducible DRE occupancy (18) and implies that, in RWPE-1 cells, DREs 3 and 6 are functionally active and are occupied by AhRC in response to TCDD. In contrast, in LNCaP cells treated with TCDD, we do not detect any changes in the DMS modification pattern and therefore infer that DREs 3 and 6 remain unoccupied. In LNCaP cells cotreated with 5-aza-CdR and TCDD, we observe a slight change in the DMS modification pattern consistent with partial DRE occupancy (Fig. 4*A* and *B*). This partial DRE occupancy is consistent with the partial restoration of *CYP1A1* mRNA inducibility observed in LNCaP cells cotreated with TCDD and 5-aza-CdR (Fig. 1). Together, these findings show that DREs 3 and 6, although unmethylated, are functionally inactive in LNCaP cells and that inhibition of DNA methylation partially restores their activity. Because DNA methylation cannot directly block AhRC binding at these sites, we conclude that it acts indirectly to inhibit AhRC access.

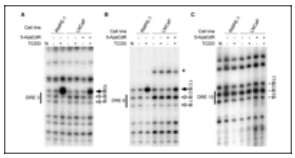

View larger version:
In this page In a new window
Download as PowerPoint Slide

Figure 4.

In vivo footprinting of AhRC-binding sites. Cells treated with 5-aza-CdR (1 μmol/L) for 7 days and/or TCDD (10 nmol/L) for 2 hours were analyzed by *in vivo* footprinting as described previously (13, 14). *N,* naked genomic DNA treated with DMS *in vitro* was also analyzed. *Filled arrows,* sites hypersensitive to DMS modification following DRE occupancy; *open arrows,* sites hyposensitive to DMS modification following DRE occupancy. *Dashes,* sites that are unaffected by TCDD treatment. Location and sequence of the DRE sites are shown. *Bold font,* guanine residues that are reactive with DMS. *Asterisk,* a DMS sensitive site present in LNCaP cells but not in RWPE-1 cells, likely representing a single nucleotide polymorphism. *A,* analysis of DRE 3. *B,* analysis of DRE 6. *C,* analysis of DRE 10. These experiments were repeated twice with similar results.

We next analyzed DRE 10, a site upstream of the *CYP1A1* enhancer that is highly methylated in both LNCaP and RWPE-1 cells (Fig. 3*D*). Here, we do not observe any TCDD-inducible change in the DMS modification pattern in either cell type (Fig. 4*C*). This observation is consistent with the findings of Kress et al. (18). We conclude that DRE 10 does not bind protein *in vivo* and is therefore nonfunctional.

We also analyzed DREs 4 and 5, sites that are highly methylated in LNCaP cells but not in RWPE-1 cells (Fig. 3*D*). In RWPE-1 cells, we observe a TCDD-dependent change in the DMS modification pattern consistent with AhRC binding (data not shown). Therefore, DREs 4 and 5 are functional in noncancerous human prostate cells. However, in LNCaP cells, we cannot detect a TCDD-dependent change in the DMS modification pattern even after the cells have been cotreated with 5-aza-CdR for 7 days (data not shown). We observe that this level of 5-aza-CdR treatment decreases DNA methylation at these sites by ~15% (data not shown). Therefore, at these sites, DNA methylation likely exerts both a direct effect that prevents AhRC binding in addition to its indirect effect noted above.

Effect of TCDD and DNA methylation on chromatin structure. We suspected that the indirect effect associated with DNA methylation that prevents AhRC binding might be related to the local chromatin structure. Some chromatin configurations, such as histone hyperacetylation and methylation of lysine 4 on histone H3 (H3K4), are associated with transcriptionally active genes and an accessible chromatin structure. Other chromatin configurations, such as histone hypoacetylation and methylation of lysine 9 of histone H3 (H3K9), are associated with silenced genes and a relatively inaccessible chromatin structure (19–28). Using ChIP methodology, we analyzed the chromatin structure of key regulatory regions within CpG island 1 and flanking DNA sequences (Fig. 5).

Figure 5.

Chromatin structure of the *CYP1A1* regulatory region. *A,*

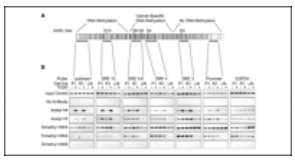

View larger version:
In this page In a new window
Download as PowerPoint Slide

CYP1A1 gene depicting CpG sites (*vertical black lines*), CpG island 1 (*gray shading*) AhRC-binding sites, DNA methylation status, and regions analyzed by ChIP (*horizontal black lines*). *B,* analysis of *CYP1A1* chromatin structure. PWR-1E (*P1*), RWPE-1 (*R1*), and LNCaP (*LN*) cells were either treated or untreated with TCDD (10 nmol/L) for 90 minutes. Cells were then used for ChIP analysis as described in Materials and Methods using the indicated antibodies. ChIP-purified DNA was amplified by PCR using primers specific for the indicated regions. PCR reactions were separated by electrophoresis on a 3% agarose gel and stained with ethidium bromide. This experiment was repeated twice with similar results.

In dioxin-responsive PWR-1E and RWPE-1 cells, TCDD treatment increases the acetylation of histones H3 and H4 on the *CYP1A1* promoter (Fig. 5*B*). This finding is consistent with previous reports (29, 30) and is likely due to AhRC's recruitment of proteins with histone acetyltransferase (HAT) activity (31). We also detect TCDD increased histone acetylation in the heavily methylated DNA region upstream of the regulatory elements of *CYP1A1* (Fig. 5*B, DRE 10* and *upstream*). This finding shows that the HAT activity recruited by AhRC does not target the *CYP1A1* promoter with specificity and that it can modify histones associated with methylated DNA. We do not observe a TCDD-dependent change in histone acetylation in LNCaP cells; this finding is expected due to the inability of AhRC to bind to the *CYP1A1* enhancer (Fig. 4). Importantly, we do not detect any cell line–specific differences in the basal level of histone acetylation in the vicinity of DRE 3. Therefore, histone H3 and H4 acetylation is not associated with the inability of AhRC to bind to DRE 3 in LNCaP cells.

In contrast to our results assessing histone acetylation, we do not detect a TCDD-inducible increase in the level of H3K4 methylation (both dimethylated and trimethylated forms) on *CYP1A1* (Fig. 5*B*). We note a slight but significant TCDD-dependent decrease in H3K4 methylation in the vicinity of some DREs in the dioxin-responsive cell lines. This finding is consistent with that of Kim et al. (32), who report that H3K4 methylation is decreased on an activated enhancer. In LNCaP cells, there is less H3K4 methylation in the cancer-specific DNA methylation region than in the noncancerous cell lines (Fig. 5*B, DRE 4* and *DRE 5-6*). We also observe less H3K4 methylation in the methylated region of the *CYP1A1* gene relative to the nonmethylated region in the noncancerous cell lines (compare the band intensity of dimethylated and trimethylated H3K4 relative with the input control in the upstream and the promoter panels). Together, these data indicate that H3K4 methylation is decreased in regions containing methylated DNA.

Surprisingly, we find striking differences in the levels of dimethyl H3K4 and trimethyl H3K4 within the *CYP1A1* regulatory region (Fig. 5*B*). Dimethyl H3K4 is prevalent and present at approximately equal levels on the *CYP1A1* promoter and DRE 3 region in all cell types. In contrast, trimethyl H3K4 is found at much lower levels in these regions in LNCaP cells relative to PWR-1E and RWPE-1 cells. These data show that, on

CYP1A1, trimethyl H3K4 levels are depleted beyond the methylated DNA region, whereas dimethyl H3K4 levels are depleted specifically within the methylated DNA region.

Dimethyl H3K9 is associated with inactive genes and heterochromatin; we cannot detect this histone modification on *CYP1A1* in appreciable amounts in any cell line. We therefore conclude that dimethyl H3K9 is not associated with *CYP1A1* expression in human prostate cells.

***CYP1A1* enhancer methylation in human prostate tissue.** Finally, we analyzed *CYP1A1* enhancer methylation in DNA isolated from 30 cancerous and 30 noncancerous human prostate tissue samples by bisulfite DNA sequencing and estimated the methylation level based on four categories: undetectable (<5%), low (5-20%), moderate (20-50%), and heavy (>50%). We could not detect *CYP1A1* enhancer methylation in any of the DNA samples isolated from noncancerous prostate tissue (data not shown). In contrast, we detect *CYP1A1* enhancer methylation in 36% (11 of 30) of the DNA samples isolated from prostate tumors (Fig. 6). This finding shows that the *CYP1A1* enhancer is aberrantly hypermethylated in human prostate cancer. Within the 11 positive DNA samples, the pattern and extent of *CYP1A1* enhancer methylation varies considerably (Fig. 6). Two DNA samples (samples 20 and 21) exhibit only low methylation of an isolated CpG site; we feel that it is unlikely that this pattern of methylation will significantly affect gene expression. All of the nine remaining DNA samples exhibit significant methylation of several CpG sites. Three samples (samples 28-30) exhibit a DNA methylation pattern whose extent approaches that observed in LNCaP cells. Extrapolating from our previous results, these tumors are likely suppressed in their ability to induce *CYP1A1* in response to dioxin.

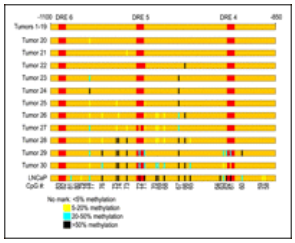

View larger version:
In this page In a new window
Download as PowerPoint Slide

Figure 6.

CYP1A1 gene methylation in human prostate tissue. Pattern and extent of CpG methylation in individual prostate tumors. Individual CpG sites are identified by the numbering system presented in Fig. 2*B*. *Red boxes,* AhRC-binding sites. Extent of CpG methylation was estimated by direct bisulfite DNA sequencing. *No mark,* <5% methylation; *yellow line,* 5% to 20% methylation; *blue line,* 20% to 50% methylation; *black line,* >50% methylation. No methylation is detected in 30 noncancerous prostate samples and in prostate tumors 1 to 19. Pattern and extent of DNA methylation observed in LNCaP cells as estimated by the direct sequencing of PCR products is also presented.

Discussion

Dioxin is a notorious environmental contaminant that is highly toxic to experimental animals and is classified as a group 1 human carcinogen by the IARC. This classification, however, is controversial, and the risk that dioxin poses to human health is uncertain (4– 6). Clearly, continued work analyzing dioxin action in humans is necessary to resolve this important issue.

Transcriptional induction of *CYP1A1* is a widely used model system to study mechanistic aspects of dioxin action (7). In this study, we analyze the effects of DNA methylation on *CYP1A1* induction and dioxin action in cultured human prostate cells and in human prostate tissue samples. The prostate gland is highly sensitive to dioxin. Studies in rats show that dioxin induces *CYP1A1* in prostate tissue and elicits adverse developmental effects (33– 36). In humans, there is limited/suggestive evidence of an association between dioxin exposure and prostate cancer (37). We find that, in LNCaP cells, a cancerous prostate cell line, dioxin induction of *CYP1A1* is severely repressed by DNA methylation. In addition, in human prostate tumors, the *CYP1A1* enhancer is aberrantly hypermethylated. Importantly, some prostate tumors exhibit a pattern of DNA methylation similar to that observed in LNCaP cells (Fig. 6). These tumors are likely impaired in their ability to induce *CYP1A1* in response to dioxin.

In our study, we determine the methylation status of all CpG sites within and flanking a CpG island that encompasses the *CYP1A1* regulatory region. Interestingly, we find that within the CpG island DNA methylation is not uniform and falls into distinct domains that closely align with regulatory function. CpG sites 1 to 36 are not methylated in cancerous and noncancerous cells. This DNA region contains the *CYP1A1* promoter and is responsible for correct initiation of gene transcription. CpG sites 37 to 90 exhibit cancer-dependent hypermethylation. This DNA region corresponds to the *CYP1A1* enhancer and mediates TCDD inducibility. CpG sites 91 to 125 are methylated in cancerous and noncancerous cells. There is no known regulatory function associated with this DNA region, possibly due to its positive methylation status. Future studies to determine mechanisms that control such differential DNA methylation can provide useful insights in the field of cancer-related epigenetics.

Previous *in vitro* studies reveal that methylation of the internal CpG site within the DRE motif inhibits AhRC binding in an electrophoretic mobility shift assay and suppresses TCDD-inducible reporter gene activity (9, 10). These findings show that DNA methylation directly inhibits DRE function. Our *in vivo* studies analyzing DREs 3 and 6 in LNCaP cells show that, although the DREs are not methylated, they are functionally inactive. Significantly, treatment of LNCaP cells with a DNA methylation inhibitor leads to partial restoration of DREs 3 and 6 function and partial restoration of *CYP1A1* inducibility. These findings indicate that DNA methylation can act indirectly to inhibit DRE function.

Trimethyl H3K4 is exclusively associated with active genes (22, 23). Our ChIP experiments show that, in LNCaP cells, trimethyl H3K4 is dramatically depleted in the DNA regions containing DREs 3 and 6. This altered chromatin structure is likely associated with the inability of AhRC to interact with these sites and, thus, possibly represents the indirect effect associated with DNA methylation that renders the DNA nonfunctional. Recent reports show that specific proteins catalyze H3K4 trimethylation and that histone demethylation is dynamically regulated (38– 43). We envision that DNA methylation depletes trimethyl H3K4 to generate a repressive, inaccessible chromatin structure. Depletion of H3K4 might be accomplished by inhibiting H3K4 trimethylation or by inducing a demethylase specific for trimethyl H3K4. Future studies that explore the relationship between DNA methylation, chromatin structure, and DNA accessibility will provide insights into these intriguing possibilities.

Our finding that *CYP1A1* is aberrantly hypermethylated in prostate cancer is novel. This finding adds *CYP1A1* to an expanding list of genes that display hypermethylation in prostate tumors (44, 45). It is unclear if *CYP1A1* hypermethylation is restricted to prostate cancer or if the gene is hypermethylated in cancers at other sites. A study analyzing human lung tissue indicates that *CYP1A1* methylation is not altered in lung cancer (11). In cell line studies, the *CYP1A1* enhancer exhibits partial methylation in human MCF-7 and HeLa cells (12). In addition, cultured rabbit kidney and lung cells display partial *CYP1A1* enhancer methylation (10). Future work analyzing *CYP1A1* methylation in other organs may provide insight into tissue-specific and cancer-related regulation of *CYP1A1* gene expression.

CYP1A1 encodes a cytochrome *P*450 that metabolizes polycyclic aromatic hydrocarbons and contributes to both their detoxification and, paradoxically, their bioactivation into toxic and mutagenic intermediates (5). It is currently unclear if *CYP1A1* induction has a positive or negative effect toward animal health (46). Therefore, the medical significance of our finding that *CYP1A1* induction is compromised in some prostate tumors is unclear.

Acknowledgments

Grant support: NIH grants RO1AG21418, RO1CA1018447, and T32DK07790; Veterans Affairs Merit Review Award; and Veterans Affairs Research Enhancement Award Program.

The costs of publication of this article were defrayed in part by the payment of page charges. This article must therefore be hereby marked *advertisement* in accordance with 18 U.S.C. Section 1734 solely to indicate this fact.

We thank Henry Tse for technical assistance.

Footnotes

Received February 8, 2006.
Revision received June 1, 2006.
Accepted June 2, 2006.

References

1. Baylin SB. Mechanisms underlying epigenetically mediated gene silencing in cancer. *Semin Cancer Biol* 2002; **12**: 331–7.
   CrossRef Medline
2. Jones PA, Baylin SB. The fundamental role of epigenetic events in cancer. *Nat Rev Genet* 2002; **3**: 415–28. Medline
3. Esteller M. Aberrant DNA methylation as a cancer-inducing mechanism. *Annu Rev Pharmacol Toxicol* 2005; **45**: 629–56.
   CrossRef Medline
4. IARC Working Group on the Evaluation of Carcinogenic Risks to Humans: Polychlorinated Dibenzo-Para-Dioxins and Polychlorinated Dibenzofurans. Lyon, France, 4-11 February 1997. *IARC Monogr Eval Carcinog Risks Hum* 1997; **69**: 1–631.
   Medline
5. Poland A, Knutson JC. 2,3,7,8-Tetrachlorodibenzo-*p*-dioxin and related halogenated aromatic hydrocarbons: examination of the mechanism of toxicity. *Annu Rev Pharmacol Toxicol* 1982; **22**: 517–54. CrossRef Medline
6. Cole P, Trichopoulos D, Pastides H, Starr T, Mandel JS. Dioxin and cancer: a critical review. *Regul Toxicol Pharmacol* 2003; **38**: 378–

88. CrossRef Medline

7. Whitlock JP, Jr. Induction of cytochrome P4501A1. *Annu Rev Pharmacol Toxicol* 1999; **39**: 103–25. CrossRef Medline
8. Swanson HI, Chan WK, Bradfield CA. DNA binding specificities and pairing rules of the Ah receptor, ARNT, and SIM proteins. *J Biol Chem* 1995; **270**: 26292–302. Abstract/FREE Full Text
9. Shen ES, Whitlock JP, Jr. The potential role of DNA methylation in the response to 2,3,7,8-tetrachlorodibenzo-*p*-dioxin. *J Biol Chem* 1989; **264**: 17754–58. Abstract/FREE Full Text
10. Takahashi Y, Suzuki C, Kamataki T. Silencing of CYP1A1 expression in rabbits by DNA methylation. *Biochem Biophys Res Commun* 1998; **247**: 383–6. CrossRef Medline
11. Anttila S, Hakkola J, Tuominen P, et al. Methylation of cytochrome P4501A1 promoter in the lung is associated with tobacco smoking. *Cancer Res* 2003; **63**: 8623–8. Abstract/FREE Full Text
12. Nakajima M, Iwanari M, Yokoi T. Effects of histone deacetylation and DNA methylation on the constitutive and TCDD-inducible expressions of the human CYP1 family in MCF-7 and HeLa cells. *Toxicol Lett* 2003; **144**: 247–56. CrossRef Medline
13. Wu L, Whitlock JP, Jr. Mechanism of dioxin action: Ah receptor-mediated increase in promoter accessibility *in vivo*. *Proc Natl Acad Sci U S A* 1992; **89**: 4811–5. Abstract/FREE Full Text
14. Okino ST, Whitlock JP, Jr. Dioxin induces localized, graded changes in chromatin structure: implications for Cyp1A1 gene transcription. *Mol Cell Biol* 1995; **15**: 3714–21. Abstract/FREE Full Text
15. Karpf AR, Jones DA. Reactivating the expression of methylation silenced genes in human cancer. *Oncogene* 2002; **21**: 5496–503. CrossRef Medline
16. Issa JP, Kantarjian H. Azacitidine. *Nat Rev Drug Discov* 2005; **Suppl**: S6–7.
17. Takai D, Jones PA. The CpG island searcher: a new WWW resource. *In Silico Biol* 2003; **3**: 235–40. Medline
18. Kress S, Reichert J, Schwarz M. Functional analysis of the human cytochrome P4501A1 (CYP1A1) gene enhancer. *Eur J Biochem* 1998; **258**: 803–12. Medline
19. Santos-Rosa H, Caldas C. Chromatin modifier enzymes, the histone code and cancer. *Eur J Cancer* 2005; **41**: 2381–402. CrossRef Medline
20. Lachner M, Jenuwein T. The many faces of histone lysine methylation. *Curr Opin Cell Biol* 2002; **14**: 286–98. CrossRef Medline
21. Fischle W, Wang Y, Allis CD. Histone and chromatin cross-talk. *Curr Opin Cell Biol* 2003; **15**: 172–83. CrossRef Medline
22. Santos-Rosa H, Schneider R, Bannister AJ, et al. Active genes are tri-methylated at K4 of histone H3. *Nature* 2002; **419**: 407–11. CrossRef Medline
23. Schneider R, Bannister AJ, Myers FA, Thorne AW, Crane-Robinson C, Kouzarides T. Histone H3 lysine 4 methylation patterns in higher eukaryotic genes. *Nat Cell Biol* 2004; **6**: 73–7. CrossRef Medline
24. Strahl BD, Allis CD. The language of covalent histone modifications. *Nature* 2000; **403**: 41–5. CrossRef Medline
25. Jenuwein T, Allis CD. Translating the histone code. *Science* 2001; **293**: 1074–80. Abstract/FREE Full Text
26. Turner BM. Cellular memory and the histone code. *Cell* 2002; **111**: 285–91. CrossRef Medline
27. Wang G, Liu T, Wei LN, Law PY, Loh HH. DNA methylation-related

chromatin modification in the regulation of mouse δ-opioid receptor gene. *Mol Pharmacol* 2005; **67**: 2032–9. **Abstract/FREE Full Text**

28. Nguyen CT, Gonzales FA, Jones PA. Altered chromatin structure associated with methylation-induced gene silencing in cancer cells: correlation of accessibility, methylation, MeCP2 binding, and acetylation. *Nucleic Acids Res* 2001; **29**: 4598–606. **Abstract/FREE Full Text**

29. Matthews J, Wihlen B, Thomsen J, Gustafsson JA. Aryl hydrocarbon receptor-mediated transcription: ligand-dependent recruitment of estrogen receptor α to 2,3,7,8-tetrachlorodibenzo-*p*-dioxin-responsive promoters. *Mol Cell Biol* 2005; **25**: 5317–28. **Abstract/FREE Full Text**

30. Ke S, Rabson AB, Germino JF, Gallo MA, Tian Y. Mechanism of suppression of cytochrome P-450 1A1 expression by tumor necrosis factor-α and lipopolysaccharide. *J Biol Chem* 2001; **276**: 39638–44. **Abstract/FREE Full Text**

31. Hankinson O. Role of coactivators in transcriptional activation by the aryl hydrocarbon receptor. *Arch Biochem Biophys* 2005; **433**: 379–86. **CrossRef** **Medline**

32. Kim J, Jia L, Tilley WD, Coetzee GA. Dynamic methylation of histone H3 at lysine 4 in transcriptional regulation by the androgen receptor. *Nucleic Acids Res* 2003; **31**: 6741–7. **Abstract/FREE Full Text**

33. Roman BL, Sommer RJ, Shinomiya K, Peterson RE. *In utero* and lactational exposure of the male rat to 2,3,7,8-tetrachlorodibenzo-*p*-dioxin: impaired prostate growth and development without inhibited androgen production. *Toxicol Appl Pharmacol* 1995; **134**: 241–50. **CrossRef** **Medline**

34. Roman BL, Pollenz RS, Peterson RE. Responsiveness of the adult male rat reproductive tract to 2,3,7,8-tetrachlorodibenzo-*p*-dioxin exposure: Ah receptor and ARNT expression, CYP1A1 induction, and Ah receptor down-regulation. *Toxicol Appl Pharmacol* 1998; **150**: 228–39. **CrossRef** **Medline**

35. Ohsako S, Miyabara Y, Sakaue M, et al. Developmental stage-specific effects of perinatal 2,3,7,8-tetrachlorodibenzo-*p*-dioxin exposure on reproductive organs of male rat offspring. *Toxicol Sci* 2002; **66**: 283–92. **Abstract/FREE Full Text**

36. Ohsako S, Miyabara Y, Nishimura N, et al. Maternal exposure to a low dose of 2,3,7,8-tetrachlorodibenzo-*p*-dioxin (TCDD) suppressed the development of reproductive organs of male rats: dose-dependent increase of mRNA levels of 5α-reductase type 2 in contrast to decrease of androgen receptor in the pubertal ventral prostate. *Toxicol Sci* 2001; **60**: 132–43. **Abstract/FREE Full Text**

37. Institute of Medicine. Veterans and Agent Orange: update 1998. Washington, DC: National Academy Press; 1999.

38. Schneider J, Wood A, Lee JS, et al. Molecular regulation of histone H3 trimethylation by COMPASS and the regulation of gene expression. *Mol Cell* 2005; **19**: 849–56. **CrossRef** **Medline**

39. Bannister AJ, Kouzarides T. Reversing histone methylation. *Nature* 2005; **436**: 1103–6. **CrossRef** **Medline**

40. Wysocka J, Milne TA, Allis CD. Taking LSD 1 to a new high. *Cell* 2005; **122**: 654–8. **CrossRef** **Medline**

41. Shi YJ, Matson C, Lan F, Iwase S, Baba T, Shi Y. Regulation of LSD1 histone demethylase activity by its associated factors. *Mol Cell* 2005; **19**: 857–64. **CrossRef** **Medline**

42. Lee MG, Wynder C, Cooch N, Shiekhattar R. An essential role for CoREST in nucleosomal histone 3 lysine 4 demethylation. *Nature* 2005; **437**: 432–5. **Medline**

43. Metzger E, Wissmann M, Yin N, et al. LSD1 demethylates repressive histone marks to promote androgen-receptor-dependent

transcription. *Nature* 2005; **437**: 436–9. **Medline**

44. Li LC, Okino ST, Dahiya R. DNA methylation in prostate cancer. *Biochim Biophys Acta* 2004; **1704**: 87–102. **Medline**

45. Li LC, Carroll PR, Dahiya R. Epigenetic changes in prostate cancer: implication for diagnosis and treatment. *J Natl Cancer Inst* 2005; **97**: 103–15. **Abstract/FREE Full Text**

46. Nebert DW, Dalton TP, Okey AB, Gonzalez FJ. Role of aryl hydrocarbon receptor-mediated induction of the CYP1 enzymes in environmental toxicity and cancer. *J Biol Chem* 2004; **279**: 23847–50. **Abstract/FREE Full Text**

Articles citing this article

Changes in Expression of Drug-Metabolizing Enzymes by Single-Walled Carbon Nanotubes in Human Respiratory Tract Cells

Drug Metab. Dispos. March 1, 2012 40:579-587

Abstract **Full Text** **Full Text (PDF)**

Role of Epigenetic Mechanisms in Differential Regulation of the Dioxin-Inducible Human CYP1A1 and CYP1B1 Genes

Mol. Pharmacol. October 1, 2010 78:608-616

Abstract **Full Text** **Full Text (PDF)**

A Dioxin-Responsive Enhancer 3' of the Human CYP1A2 Gene

Mol. Pharmacol. December 1, 2007 72:1457-1465

Abstract **Full Text** **Full Text (PDF)**